

## Spectroscopy and correlations probed in direct two-nucleon knockout reactions

This content has been downloaded from IOPscience. Please scroll down to see the full text.

2012 J. Phys.: Conf. Ser. 381 012108

(<http://iopscience.iop.org/1742-6596/381/1/012108>)

View [the table of contents for this issue](#), or go to the [journal homepage](#) for more

Download details:

IP Address: 150.203.19.30

This content was downloaded on 10/06/2014 at 03:43

Please note that [terms and conditions apply](#).

# Spectroscopy and correlations probed in direct two-nucleon knockout reactions

**E C Simpson**

Department of Physics, Faculty of Engineering and Physical Sciences, University of Surrey,  
Guildford, Surrey GU2 7XH, UK

E-mail: [e.simpson@surrey.ac.uk](mailto:e.simpson@surrey.ac.uk)

**Abstract.** Nucleon knockout reactions from fast radioactive secondary beams colliding with light nuclear targets provide a useful tool for studying structure away from the valley of  $\beta$ -stability. An efficient means of producing specific exotic nuclei, the technique has been recently applied to study nuclear halos, isospin symmetry and cross-shell excitations, and in tracking the evolution of single-particle states, and probing the associated quenching ( $N=20$ ,  $N=28$ ) and emergence ( $N=16$ ) of shell gaps. Recent theoretical work has demonstrated the sensitivity of residue momentum distributions following two-nucleon removal to the underlying structure. In particular, there is a sensitivity to the total orbital angular momentum of the removed pair, providing additional tests of (shell- or many-body-) structure-model two-nucleon overlaps. We illustrate the structural sensitivities in the context of nucleon knockout from  $^{12}\text{C}$  and  $^{16}\text{O}$ , and discuss the prospects for studying np-correlations along the  $N = Z$  line, highlighting the need for new final-state exclusive measurements, including those with stable beams.

## 1. Introduction

Current and near-future international radioactive beam facilities provide the first opportunity to study many highly unstable exotic nuclei. These exhibit a wide variety of novel structural phenomena, often radically different from the template set out by nuclei in the valley of  $\beta$ -stability. Shell structure is found to evolve with increasing proton-neutron asymmetry, with the quenching of shell gaps ( $N=20$ ,  $N=28$ ) creating regions of rapidly changing structure. Examples are the island of inversion, and the emergence of the new shell gap at  $N = 16$ , giving rise to the new doubly magic nucleus  $^{24}\text{O}$ . Halo nuclei, by virtue of one or more very weakly bound nucleons, are significantly larger than stable isobars and have been discovered along the neutron dripline, the location of which will be extended upwards in mass as new facilities come online. This journey also brings us closer to the paths of the astrophysical processes that produce the heavy elements, and our understanding of nuclear structure in these regions is crucial in determining the existence of  $r$ -process waiting points and the abundances of the elements.

These phenomena, studied using low intensity radioactive beams, have required new experimental techniques and associated reaction theories to provide the interface between experiment and structure models. Here we present one such technique, two-nucleon knockout, discuss the aspects of structure probed, and consider such reactions on  $N = Z$  nuclei.

## 2. Two-nucleon knockout reactions

Fast nucleon knockout reactions, involving the removal of one or two nucleons in a collision of a (secondary) beam, of energy 80 MeV/nucleon or greater, and a light nuclear target (beryllium or carbon) are a useful tool for studying the structure of exotic nuclei. The success of the technique is in part due to its efficiency; after the reaction, only properties of the heavy reaction residue, which is typically assumed to act as a spectator in the reaction, are observed. Measurement of decay  $\gamma$ -rays provides simple spectroscopic information, which, coupled with cross section measurements, offers information on the overlap of the initial and final states. Additionally, the shapes and widths of the beam-directional momentum distributions of the heavy residues are characteristic of the angular momentum of the removed nucleons, providing further spectroscopic information [1].

The technique has been applied to study structural phenomena in exotic nuclei including nuclear haloes (e.g.  $^{15}\text{C}$  [2],  $^{19}\text{C}$  [3]), suppressed spectroscopic strengths in asymmetric nuclei [4, 5], evolution and quenching of the  $N = 28$  shell gap [6, 7], the  $N = 20$  island of inversion [8, 9], and the possibility of a new island of inversion centred on  $^{64}\text{Cr}$  [10]. A further, more recent avenue of study concerns two-nucleon removal to study proton-neutron correlations in nuclei along the  $N = Z$  line [11].

Our interest here is in the aspects of structure probed by two-nucleon knockout. Bazin *et al.* first described two-nucleon removal as a direct reaction using a simple uncorrelated model [12]. A fully correlated model taking shell-model structure input was later developed to describe inelastic [13] and elastic [14] removal of nucleons. Consideration was then given to the momentum distributions of the heavy reaction residues [15, 16]. Here we summarise aspects of the structure probed; further details may be found in the above references.

In contrast to single-nucleon removal, structural and reaction dynamical aspects do not simply factor; the contributing structure-model two-nucleon amplitudes contribute coherently. The essential structural input is the two-nucleon overlap.

$$\begin{aligned} \Psi_{J_i M_i T_i \tau_i}^{(F)}(1, 2) &\equiv \langle \Phi^{(F)}(A) | \Psi_i(A, 1, 2) \rangle \\ &= \sum_{I\mu T\alpha} C_{\alpha}^{IT} (I\mu J_f M_f | J_i M_i) (T\tau T_f \tau_f | T_i \tau_i) \overline{[\psi_{\beta_1}(1) \otimes \psi_{\beta_2}(2)]_{I\mu}^{T\tau}} \end{aligned} \quad (1)$$

Here  $\alpha$  denotes the two-nucleon configurations  $(\beta_1, \beta_2)$ , namely the quantum numbers of the two nucleons,  $\beta_1 \equiv (n_1 \ell_1 j_1)$  and  $\beta_2 \equiv (n_2 \ell_2 j_2)$ , and the square bracketed term is the antisymmetrized two-nucleon wave function.  $C_{\alpha}^{IT}$  are the signed two-nucleon amplitudes (TNA), which express the similarity of projectile initial and residue final states, and largely determine the branching to different residue final states, which are well produced using shell model amplitudes [14].

The interactions between projectile constituents and the target are typically calculated by folding the target and projectile constituent densities with an effective nucleon-nucleon interaction. These densities are taken from reaction cross section measurements or Hartree-Fock calculations. In essence, the reaction samples the square modulus of the two-nucleon overlap functions, projected onto the impact parameter plane, over an area determined by the projectile constituent-target  $S$ -matrices (see Fig. 4 of Ref. [16]). Necessarily, the two-nucleons must interact strongly with the target, but the core (reaction residue) must be sufficiently distant, so the reaction favours configurations where the two nucleons are spatially localised near the projectile surface.

In addition to the absolute magnitudes of the TNA and their relative phases, contributions from cross-shell configurations that mix opposite parity orbitals into the two-nucleon overlap, may strongly enhance or degrade two-nucleon spatial correlations (see e.g. Ref. [17]). Orbits of differing parity introduce an asymmetry into the two-nucleon density distribution (with respect to an angular separation of the nucleon position vectors  $\hat{r}_1$  and  $\hat{r}_2$  of  $90^\circ$ ) that may lead to large

increases (or decreases) in two-nucleon knockout cross sections. Similarly, simple cross-shell negative parity states could also be sensitive to the relative strengths and phases of contributing configurations, allowing one to investigate their structure in more detail.

Beam directional residue momentum distributions after the reaction are broadly characteristic of the total angular momentum of the removed nucleon pair  $\mathbf{j}_1 + \mathbf{j}_2 = \mathbf{I}$ , which in turn couples the initial and final state spins  $\mathbf{J}_f + \mathbf{I} = \mathbf{J}_i$ . Larger  $I$  produce wider momentum distributions giving the reaction mechanism some sensitivity to the spins of the final states populated. Excellent agreement with final-state-inclusive experiments has been found for  $^{22}\text{Mg}(-2n)$ , where the dominant  $0^+$  ground state leads to a narrow inclusive momentum distribution, and  $^{28}\text{Mg}(-2p)$ , where  $2^+$  and  $4^+$  states are populated giving a broader inclusive distribution [16]. Only even-even nuclei have thus far been considered in detail. Projectiles with non-zero ground state spin allow multiple couplings to populate a given residue final state. Although the immediate link between the residue momentum and final state spin is lost, the contributing  $I$  are determined by the nuclear structure input, and a given final state may yet have a characteristic momentum distribution shape and width.

Underlying this sensitivity to  $I$  in the momentum distributions, lies a sensitivity to the total orbital angular momentum  $L$ ,  $\ell_1 + \ell_2 = \mathbf{L}$ , which couples to the total spin  $S$  to give  $I$ ,  $\mathbf{L} + \mathbf{S} = \mathbf{I}$ . Again, larger  $L$  give broader residue momentum distributions [18]. The contributing  $L$  for any given final state are determined by the two-nucleon amplitudes and their relative phases, meaning that final states of the same spin may not exhibit the same momentum distributions. For example, the momentum distribution widths for the first and second  $2^+$  states in  $^{24}\text{Si}$ , populated via  $^{26}\text{Si}(-2n)$ , are expected to differ by  $\sim 25\%$ . This variation is not universal - the first and second  $2^+$  states in  $^{26}\text{Ne}$  populated via  $^{28}\text{Mg}(-2p)$  show no significant difference in width - but in particular cases may provide the leverage for novel, detailed tests of structure model amplitudes.

### 3. Two-nucleon removal from $N = Z$ nuclei

Current experimental applications of the two-nucleon knockout have focussed on the removal of two deeply-bound like-nucleons in exotic sd-shell nuclei, providing an efficient route to specific exotic isotopes and often establishing the first spectroscopic information. Such experiments push the boundaries of nuclear structure knowledge, but it is also necessary to test and verify the associated reaction theories on structurally well understood systems, including stable isotopes.

Further, knockout experiments using high energy electrons have found evidence of enhanced short-range proton-neutron correlations in light stable isotopes [19]. An interesting question therefore is whether like and unlike two-nucleon removal also exhibit any evidence of enhanced  $np$  over  $nn$  and  $pp$  spatial correlations on a longer length scale than implied by the short-range correlations observations of the electron knockout data. Here, the spatial (geometrical) selectivity of the reaction mechanism would provide the leverage and probe of the presence of spatially localized pairs and evidence of enhanced  $np$  correlations. We first consider the prospects for such measurements and then discuss two specific examples.

#### 3.1. Prospects: direct and indirect reactions

In contrast to single-nucleon removal, direct population of the reaction residue of interest is not guaranteed. Experimental studies have thus far primarily exploited the reaction mechanism to remove the deficient species, pushing further from stability, where the asymmetric nucleon separation thresholds ensure the reaction is direct [12]. The removal of two weakly bound nucleons may proceed indirectly, via single nucleon removal to particle-unbound states in the  $(A - 1)$ -body system, which subsequently emit a second nucleon, a path shown to dominate in a study on neutron-rich carbon isotopes [20]. For the present case of  $np$  removal, two indirect routes are possible, (i) the removal of a proton to populate a neutron-unbound state, and (ii)

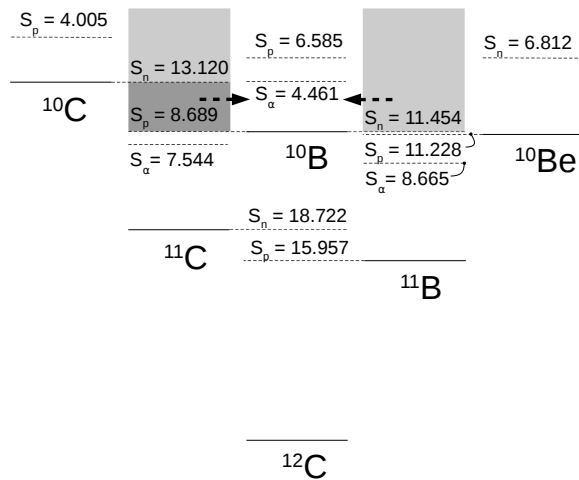


**Figure 1.** Nucleon separation thresholds relevant to nucleon knockout from  $^{12}\text{C}$ . The shaded areas highlight excitation ranges in the  $A = 11$  residues through which the  $^{10}\text{B}$  residue could be populated.

the removal of a neutron populating a proton-unbound state. In the absence of an experimental data that distinguish the evaporative contributions, the examples considered must be carefully chosen to minimise indirect contributions.

Projectiles with large and symmetric nucleon separation energies are most promising. If either species is weakly bound, one or other nucleon threshold will be low in the  $A - 1$  nucleon system, permitting indirect removal. Further, the projectile must be relatively light; a more massive core, typically assumed inert in the associated structure model calculations, provides a route to highly excited states in the  $A - 1$  residues by removal of core nucleons. The dual requirements of symmetric nucleon separation energies and low mass constrain the number of possible projectiles considerably. Here we consider two candidates; namely,  $^{12}\text{C}$  and  $^{16}\text{O}$ , the former of which was the subject of a recent study [11].

### 3.2. Knockout from $^{12}\text{C}$

Study of  $^{12}\text{C}$  is in part motivated by intriguing experimental measurements - fragmentation cross sections for  $^{12}\text{C}$  reacting with a  $^{12}\text{C}$  target - made at the Lawrence Berkeley Laboratory Bevatron at energies of 250, 1050 and 2100 MeV/nucleon [22, 23]. These indicate that the  $np$  removal cross section is significantly larger than that for like-nucleon pairs. The larger number of active nucleons accounts for some part of the difference; assuming the simplest p-shell  $\pi[0p_{3/2}]^4\nu[0p_{3/2}]^4$  structure for  $^{12}\text{C}$ , we would expect the unlike:like two-nucleon inclusive-cross-section ratios  $\sigma_{np}/\sigma_{2N} = 16/6 \sim 2.7$ , but the data show larger enhancement than this simple combinatoric expectation. Is this additional enhancement accounted for in simple truncated-space shell model calculations? Fragment momentum distribution widths (fitted Gaussian) have also been measured [24], though the published values are averaged over different targets (Be,  $\text{CH}_2$ , C, Al, Cu, Ag, and Pb).

We first consider the  $^{12}\text{C}$  projectile. The proton and neutron separation energies of  $^{12}\text{C}$  are  $S_p(^{12}\text{C})=15.957$  and  $S_n(^{12}\text{C})=18.722$  MeV and the critical separation thresholds in the  $A = 11$  systems are  $S_p(^{11}\text{C})=8.689$  and  $S_n(^{11}\text{B})=11.454$  MeV (see Fig. 1). Population of states above these thresholds requires that the removed nucleon is bound by  $> 25$  MeV, and shell model calculations and results from the previous study on single-nucleon removal by Brown *et al.* suggest the single-particle ( $p$ -shell) strength is essentially exhausted below the relevant thresholds in the  $A = 11$  systems [21]. We conclude that the residue of interest,  $^{10}\text{B}$ , should be populated in a predominantly direct fashion.

Structure input, in the form of two-nucleon amplitudes, is taken from Oxbash [25] shell model calculations using the WBP [26] interaction in a  $p$ -shell model space. In addition to  $np$  removal

**Table 1.** Table of measured and calculated cross sections (in mb) and (gaussian fitted) momentum distribution widths for the  $A = 10$  residues following two-nucleon removal from  $^{12}\text{C}$  at 2100 MeV/nucleon. Cross sections are inclusive with respect to the residue final states.

Residue	$^{10}\text{C}$		$^{10}\text{Be}$		$^{10}\text{B}$	
	exp.	th.	exp.	th.	exp.	th.
$\sigma_{-2N}$ (mb)	4.11±0.22	5.04	5.81±0.29	6.52	35.1±3.4	19.02
Width (MeV/c)	121±6	120	129±4	127	134±3	132

we also consider the like-nucleon removal residues,  $^{10}\text{C}$  and  $^{10}\text{Be}$ . The inclusive measurements will populate both  $T = 0$  and  $T = 1$  shell model states. For each residue several states are predicted to be populated, with the first  $T = 1$ ,  $0^+$  and  $2^+$  states being common to all residues. Further details of the calculations may be found in Ref. [11].

Final-state-inclusive cross section calculations for the  $^{10}\text{C}$ ,  $^{10}\text{Be}$  and  $^{10}\text{B}$  residues are shown in Table 1 and compared to experimental measurements. Calculated theoretical like-pair removal cross sections  $\sigma_{th}$ , to  $^{10}\text{C}$  and  $^{10}\text{Be}$ , are in reasonable agreement with the experimental data of Ref. [22]. As with exotic  $sd$ -shell cases, the theoretical cross sections overestimate the experiment. However, the cross section for  $^{10}\text{B}$  is significantly underestimated by the calculation, by almost a factor of two. For comparison, the experimental  $np$  removal cross section is of the order of the single-nucleon removal cross sections,  $\sigma_{-1n} = 46.50 \pm 2.30$  and  $\sigma_{-1p} = 54.20 \pm 2.90$  mb [22]. Since the magnitudes of the  $pp$  and  $nn$  removal cross sections are reasonably described, our expectation is that the cross sections to the states of the  $T = 1$  isospin multiplet in  $^{10}\text{B}$  are similarly well determined. However, an independent measurement of these cross sections would provide a useful verification of the direct nature of the reaction. Within the direct reaction model used, we must attribute the cross-section deficit to the calculated yields of the  $T = 0$  final states.

The inclusive momentum distributions are in excellent agreement for all residues, though this may be fortuitous, given the target averaging for the experimental data. The final state exclusive momentum distributions (full-width half-maxima) form a distinct pattern, varying between 220 and 420 MeV/c. New measurements would provide a rigorous test of the reaction mechanism, with any indirect population, from either  $p$ -shell or deeply bound  $s$ -wave nucleons, being apparent. Additionally, some sensitivity to the underlying structure is expected - the momentum distribution of the first  $T = 0$ ,  $J^\pi = 1^+$  state is predicted to be significantly narrower than that of the second, and the first  $T = 0$ ,  $2^+$  and  $3^+$  states should have very similar shapes - providing further tests the of shell model wave functions used.

### 3.3. Knockout from $^{16}\text{O}$

A further candidate projectile is  $^{16}\text{O}$ , the subject of measurements at 2100 MeV/nucleon [22, 24], and also having a large  $np$  removal cross section relative to  $pp$  and  $nn$ . As with  $^{12}\text{C}$  the nucleon separation thresholds are large and approximately symmetric, with  $S_p(^{16}\text{O})=12.127$  and  $S_n(^{16}\text{O})=15.664$  MeV, and the single-nucleon strength is expected to be exhausted before the critical thresholds in the  $A = 15$  residues are met [21]. The two-neutron removal residue,  $^{14}\text{O}$ , is also of particular interest, as only the  $0^+$  ground state is bound. The cross section is thus small,  $1.67 \pm 0.12$  mb [22], and the corresponding momentum distribution width narrow,  $99 \pm 6$  MeV/c [24], providing a clean and stringent test of the reaction theory in a well studied system. Additionally, the cross sections may be sensitive to admixtures of cross-shell configurations [27], that may enhance the two-nucleon spatial correlations and increase the cross section.

#### 4. Summary

We have discussed aspects of nuclear structure probed via two-nucleon knockout reactions. Residue momentum distributions provide a handle on the spins in exotic nuclei, but additionally provide more subtle tests of structure models. Generally, higher-spin final states will lead to wider residue momentum distributions, but the details of the shell-model two-nucleon overlap are important in understanding the details of the residue momentum distributions.

We have considered theoretical expectations for the cross sections of two-nucleon removal reactions from  $^{12}\text{C}$  incident on a carbon target, at 2100 MeV per nucleon. The calculated inclusive cross sections for two-like-nucleon ( $T = 1$ ) removal are broadly consistent with available experimental data, whereas the calculated inclusive  $np$  pair removal cross sections underestimate the data by approximately a factor of 2. Theoretical calculations of the widths of the final-state-inclusive residue momentum distributions are, however, consistent with the available experimental data, for all channels. The discrepancy between the experiment and theoretical approach used here indicates that new experiments would be of great value. Specifically, final-state exclusive cross sections and residue momentum distributions would highlight if particular states are incorrectly described within the current model. Simultaneous measurements of the like-nucleon removal channels would provide valuable tests of the theoretical description and validation of the cross sections for  $T = 1$  states.

#### Acknowledgments

This work was supported by the UK Engineering and Physical Science Research Council (EPSRC) under Grant EP/P503892/1, and by the Science and Technology Facilities Council under Grant ST/F012012. Ongoing collaboration with Jeff Tostevin, Alex Brown, Daniel Bazin and Alexandra Gade is gratefully acknowledged.

#### References

- [1] Hansen P G and Tostevin J A 2003 *Ann. Rev. Nucl. Part. Sci.* **53** 219
- [2] Terry J R *et al.* 2004 *Phys. Rev. C* **69** 054306
- [3] Bazin D *et al.* 1995 *Phys. Rev. Lett.* **74** 3569
- [4] Gade A *et al.* 2004 *Phys. Rev. Lett.* **93** 042501
- [5] Gade A, Adrich P, Bazin D, Bowen M D, Brown B A, *et al.* 2008 *Phys. Rev. C* **77** 044306
- [6] Bastin B *et al.* 2007 *Phys. Rev. Lett.* **99** 022503
- [7] Santiago-Gonzalez D *et al.* 2011 *Phys. Rev. C* **83** 061305(R)
- [8] Gade A *et al.* 2007 *Phys. Rev. Lett.* **99** 072502
- [9] Fallon P *et al.* 2010 *Phys. Rev. C* **81** 041302(R)
- [10] Adrich P *et al.* 2008 *Phys. Rev. C* **77** 054306
- [11] Simpson E C and Tostevin J A 2011 *Phys. Rev. C* **83** 014605
- [12] Bazin D *et al.* 2003 *Phys. Rev. Lett.* **91** 012501
- [13] Tostevin J A, Podolyák G, Brown B A and Hansen P G 2004 *Phys. Rev. C* **70** 064602
- [14] Tostevin J A and Brown B A 2006 *Phys. Rev. C* **74** 064604
- [15] Simpson E C, Tostevin J A, Bazin D, Brown B A and Gade A 2009 *Phys. Rev. Lett.* **102** 132502
- [16] Simpson E C, Tostevin J A, Bazin D and Gade A 2009 *Phys. Rev. C* **79** 064621
- [17] Catara F, Insolia A, Maglione E and Vitturi A 1984 *Phys. Rev. C* **29** 1091
- [18] Simpson E C and Tostevin J A 2010 *Phys. Rev. C* **82** 044616
- [19] Subedi R *et al.* 2008 *Science* **320** 1476 (and references therein)
- [20] Simpson E C and Tostevin J A 2009 *Phys. Rev. C* **79** 024616
- [21] Brown B A, Hansen P G, Sherrill B M and Tostevin J A 2002 *Phys. Rev. C* **65** 061601(R)
- [22] Lindstrom P J, Greiner D E, Heckman H H, Cork B and Bieser F S 1975 LBL Preprint 3650
- [23] Kidd J M, Lindstrom P J, and Crawford H J and Woods G 1988 *Phys. Rev. C* **37** 2613
- [24] Greiner D E, Lindstrom P J, Heckman H H, Cork B and Bieser F S 1975 *Phys. Rev. Lett.* **35** 152
- [25] Brown B A, Etchegoyen A, Godwin N S, Rae W D M, Richter W A, Ormand W E, Warburton E K, Winfield J S, Zhao L and Zimmerman C H MSU-NSCL report number 1289
- [26] Warburton E K and Brown B A 1992 *Phys. Rev. C* **46** 923
- [27] Warburton E K, Brown B A and Millener D J 1992 *Phys. Lett. B* **293** 7